Solar Energy Materials & Solar Cells 100 (2012) 251–257

Contents lists available at SciVerse ScienceDirect

Solar Energy Materials & Solar Cells

journal homepage: www.elsevier.com/locate/solmat

Improved electrochromic performance of ordered macroporous tungsten oxide films for IR electrochromic device

Lili Yang [a], Dengteng Ge [b], Jiupeng Zhao [c], Yanbo Ding [c], Xiangping Kong [c], Yao Li [b,*]

[a] School of Transportation Science and Engineering, Harbin Institute of Technology, Harbin 150090, PR China
[b] Center for Composite Materials and Structures, Harbin Institute of Technology, Harbin 150080, PR China
[c] School of Chemical Engineering and Technology, Harbin Institute of Technology, Harbin 150001, PR China

ARTICLE INFO

Article history:
Received 27 September 2011
Received in revised form
20 January 2012
Accepted 24 January 2012
Available online 17 February 2012

Keywords:
WO_3 thin films
Ordered macroporous
Electrochromic properties
Near infrared

ABSTRACT

Electrochromic performance of tungsten oxide (WO_3) has attracted extensive interest due to its applications in smart windows, spacecraft thermal control and other optical devices. Here we report ordered macroporous WO_3 thin films prepared by the template-assisted sol–gel method. The principle finding of the paper is that the ordered multi-layer interconnected porous structure facilitates the diffusion of ions/electrons as well as the light transmission. Consequently we see improved IR optical modulation and faster response time in the macroporous WO_3 films. Moreover, both small pore size and perfection of ordered porous structure contribute to the improved electrochromic performance. These results have obvious practical relevance for fast near IR electrochromic devices exemplified by aerospace thermal control systems.

1. Introduction

Since late 1980s electrochromic (EC) materials have been receiving substantial attention both in science and in industry [1] due to their optical modulation in visible or infrared (IR) regions [2,3]. EC devices based on lithium intercalation in transition metal oxide films have a variety of potential applications such as energy-efficient smart windows, display devices, switchable mirrors and photoelectrochromic devices. The performance of EC devices in visible wavelength range for civil applications has been extensively studied [4]. Further research is needed in IR optical modulation with the increasing technological demands from different technologies. To the best of our knowledge, tungsten oxide (WO_3) is one of the most promising material for spacecraft thermal control or military camouflage against IR sensors due to its chemical stability and UV radiation resistance [5]. Sauvet and Hale et al. found that tungsten oxide had strong optical modulation in mid-infrared and long-infrared wavelength bands [6–9]. However, the research about near IR optical performance of tungsten oxide for spacecraft thermal control is still rare.

Recently different porous microstructures have been made on the basis of tungsten oxide to improve its EC performance, such as nanowires and mesopores [10,11]. The enhanced EC performance was attributed to the better penetration of electrolytes into the WO_3 framework and shortening of diffusion distance for lithium ions in porous films. Here we present the tungsten oxide films with three-dimensional ordered macroporous (3DOM) structure fabricated through the template-assisted sol–gel method. The benefits of 3DOM materials have been demonstrated in great accessible surface areas, well-interconnected pores and periodic structures, which could control the light transmission [12,13]. Sumida et al. [14] and Kuai et al. [15] prepared ordered macroporous WO_3 films through the electrodeposition method or the dip-infiltrating sol–gel technique, but only the tunable photonic performance due to the ion intercalation was studied. 3DOM tungsten oxide with higher photocatalytic activity was also represented in the paper of Sadakane et al. [16]. In this work, effects of ordered macroporous structure on their electrochromic properties were studied. It was found that the near IR electrochromic properties were significantly enhanced, including faster response time and greater coloration efficiency (CE). Here ordered macroporous WO_3 films were proved to have excellent potential applications in IR electrochromic device for space thermal control.

2. Experimental

2.1. Synthesis of precursor sols and polystyrene (PS) templates

The precursor solutions were prepared according to Krasovec et al. [17]. 4.6 g of metallic tungsten powder was dissolved in

* Corresponding author.
E-mail address: liyao@hit.edu.cn (Y. Li).

0927-0248/$ - see front matter © 2012 Elsevier B.V. All rights reserved.
doi:10.1016/j.solmat.2012.01.028

25 ml of H_2O_2 (30%) for 24 h. Unreacted H_2O_2 was removed using platinum net. After the addition of ethanol (20 ml), the solution was allowed to evaporate (80 °C) until the sol turned from a milky to a transparent orange color. The sol could be kept in refrigerator (4 °C) for several months.

Monodispersed PS latex spheres (diameters of 325, 410 and 620 nm) were obtained using an emulsifier-free emulsion polymerization technique [18]. Fluorine doped tin oxide (FTO) substrates (1 cm × 3 cm) were ultrasonically cleaned in acetone, ethanol and distilled water for 20 min, separately. PS colloidal crystals were grown using a controlled vertical drying method [18]. FTO glass substrates were placed into cylindrical vessels vertically. Then PS dispersion diluted to 1.0 wt% was added into the vessels and evaporated in an incubator at a stable temperature of 60 °C.

2.2. Preparation of 3DOM tungsten oxide films

The substrate with templates was dipped into the sol and slowly withdrawn at the rate of 18 cm min^{-1} at room temperature. This was followed by drying the sample at 80 °C for half an hour. The same dipping and drying process were repeated 4 times. The resulting films were dried at 40 °C for 48 h and immersed into tetrahydrofuran (THF) for 1 h to remove the PS spheres. Finally all films were annealed at 150 °C (ramp of 2 °C min^{-1}) in air and held for 2 h and then brought back to room temperature. For the sake of comparison, a tungsten oxide film without templates under the same preparation parameters and a porous film annealed at 450 °C (ramp of 2 °C min^{-1}) were also obtained.

2.3. Characterization

Samples were coated with platinum and observed on a QUANTA 200 F (FEI, America) at an accelerating voltage of 20 kV. X-ray diffraction (XRD) measurements were conducted using monochromatic Cu-Kα radiation with D/MAX2200 diffractometer (Rigaku, Japan). The X-ray photoelectron spectroscopy (XPS) measurements were recorded on a PHI5700 with a monochromatic Al-Kα X-ray source at a power of 200 W/12 kV. Binding energies for the high resolution spectra were calibrated by setting C1s at 285.0 eV. The reflection and transmission spectra were achieved from UV–vis–NIR fiber optic spectrometer (Ocean Maya 2000-Pro). The incident light was perpendicular to the surface of samples.

The electrochemical behavior was studied with cyclic voltammetry (CV) which was performed in an electrolyte solution (1 M $LiClO_4$ in propylene carbonate). The CV measurements were performed at room temperature between +1.0 and −1.0 V at scan rate of 5 mV s^{-1}. WO_3 films, Pt foil and Ag/AgCl/KCl were used as the working electrode, counter electrode and the reference electrode, respectively. The electrochromic character was performed on the combination of CHI 600D (CH Instrument Co. Ltd.) and UV–vis–NIR fiber optic spectrometer (MAYA 2000-Pro, Ocean Optics). The transmission spectra of films in the fully colored and bleached states were measured after the films have been subjected to CV activation for 15 cycles. The response time is defined as the time required by the system to change 90% of the total transmittance variation.

3. Results and discussion

3.1. Morphologies and structural characterization

Fig. 1 shows the typical top-viewed SEM micrographs of PS templates (a) and WO_3 inverse opals (b). PS templates reveal good ordering in close packed arrays while WO_3 inverse opals present ordered hexagonal macroporous with three dark "windows" inside each pore. The perfection of ordered macroporous structure gets better as the pore size increases. The center-to-center distance of PS spheres and ordered macropores are obtained as

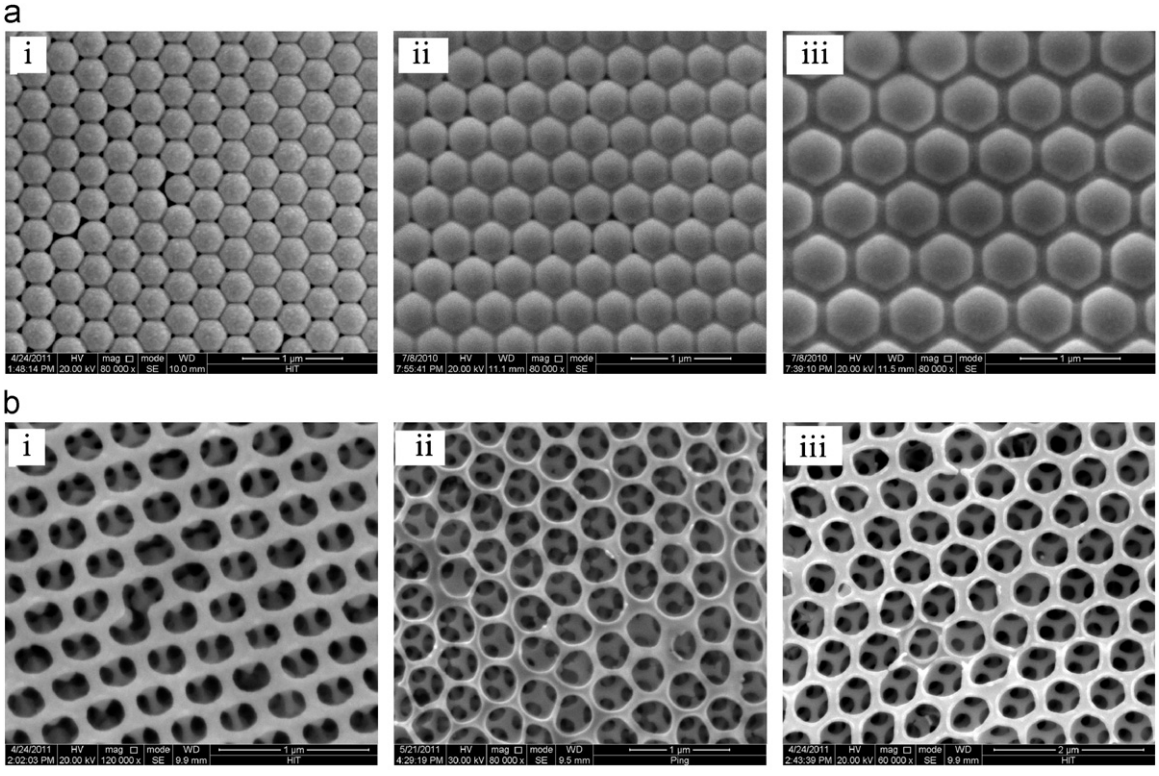

Fig. 1. SEM graphs of PS templates with different size of spheres (a) and corresponding ordered macroporous WO3 films (b).

325, 415, 635 nm and 330, 420, 615 nm, respectively. This indicates deformation or shrinkage during the removal of PS spheres or under low temperature thermal treatments. Fig. 2 shows the top-viewed micrographs of all the films' interfaces. These three kinds of macroporous films approximately have the same thickness of 2.0 ± 0.2 μm, which is about four times as that of dense tungsten oxide film (520 nm). Thus the macroporous films almost have the same solid volume as the dense films, which makes the electrochromic properties of these films comparable.

The X-ray diffractograms of WO_3 films with pore size of 325 nm under low (150 °C) and high thermal (450 °C) treatments are presented in Fig. 3. It is observed that just the tetragonal cassiterite structure of FTO (JCPDS 77-0447) is shown, so WO_3 films exhibit amorphous under low temperature. The XRD curve of WO_3 films after thermal treatments at 450 °C shows the monoclinic structure (JCPDS 43-1035) from the three strong peaks of (200), (002) and (202). Thus, the crystalline structure of tungsten oxide films appears under high thermal treatments. Previous reports have shown a decrease of coloration efficiency (CE) as amorphous WO_3 films crystallize into large particles during the annealing procedure [19,20]. The amorphous films were used as samples in following studies.

To get data on the colored and bleached states of WO_3 films, their oxidation states were analyzed by XPS. Fig. 3b and c shows the narrow-scan spectra of *W* 4f of bleached and colored WO_3, respectively. In Fig. 3b, the observed *W* 4f consisted of a single doublet at binding energies of 35.8 eV for *W* $4f_{7/2}$ and 37.9 eV for *W* $4f_{5/2}$. It can be reasoned that tungsten is present in the W^{VI} oxidation state of the bleached WO_3 films. After the coloration process, a multi-peak overlapping of *W* 4f spectra (seen in Fig. 3c) indicates that tungsten in the colored WO_3 films is multivalent. Based on the W^{V} 4f binding energies of 35 eV and 37 eV, the fitted spectra after peak separation is derived (also in Fig. 3c). Calculated from the shape of each spectrum and the area under the peaks, W^{VI} was close to 46% and W^{V} accounts for 54%.

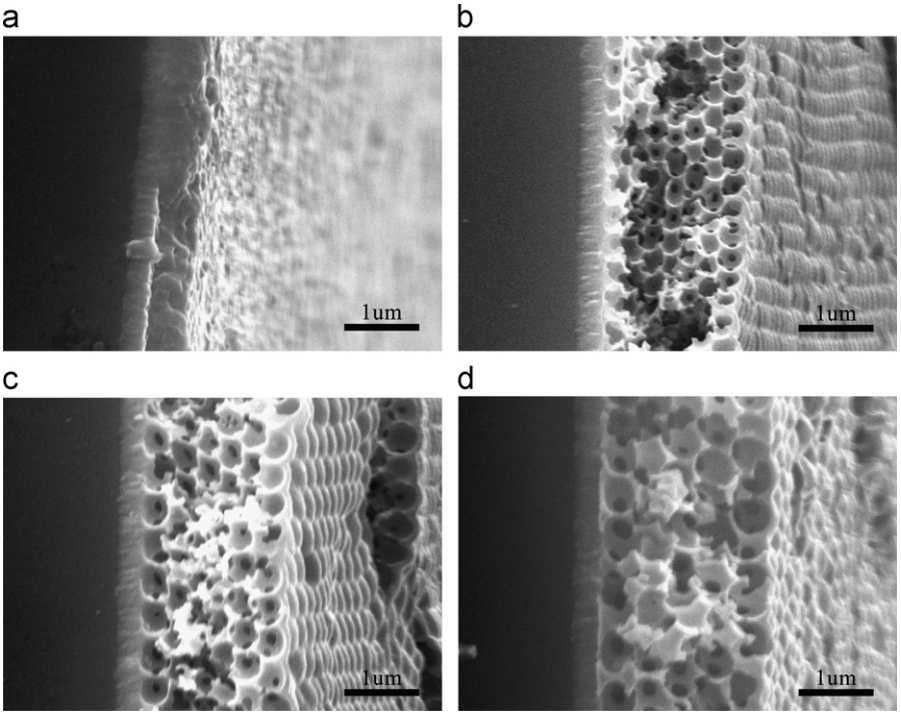

Fig. 2. SEM of dense tungsten oxide film (*a*) and macroporous WO_3 films prepared using PS sphere size of 325 nm (*b*), 410 nm (*c*) and 620 nm (*d*).

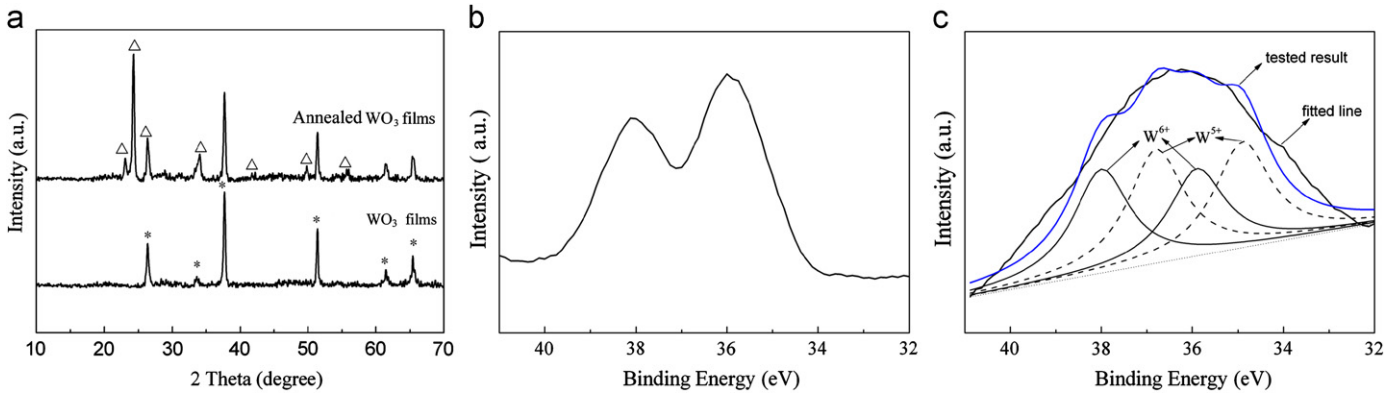

Fig. 3. XRD pattern of ordered macroporous WO_3 films (*a*) and high-resolution XPS analysis of *W* 4f of bleached (*b*) and colored WO_3 films (*c*).

The coloration-bleaching process is essentially in line with a redox process during the combinational insertion/extraction of Li^+ ions and electrons.

3.2. Electrochemical/electrochromic performance

The electrochemical/electrochromic characteristics are the most important properties of EC materials. The CV curves of the ordered macroporous and dense WO_3 films are compared in Fig. 4. Typical broad featureless peaks are shown of Li^+ insertion/extraction in amorphous WO_3. Both reduction and oxidation peaks of ordered macroporous WO_3 film are significantly stronger than those of dense films. This reflects that the ordered macroporous WO_3 films have higher insertion/extraction capacity for electrons and ions. In addition, compared with dense films, the position of oxidation peak in ordered macroporous WO_3 films is shifted from -0.539 V to -0.677 V. Therefore, it is much easier to extract the Li^+ ions during the bleaching process, which is related with the higher surface area of macroporous films.

The electrochromic performance mostly depends on the following parameters. One of them is the optical density (OD) calculated according to the following equation:

$$\Delta OD_\lambda = \log(T_{b\lambda}/T_{c\lambda}) \quad (1)$$

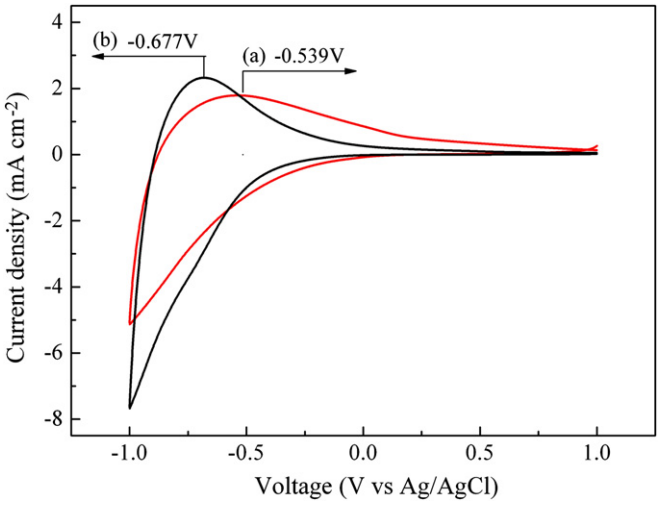

Fig. 4. Cyclic voltammograms of sol–gel derived in WO_3 films (*a*) and ordered macroporous films (*b*).

where $T_{b\lambda}$ and $T_{c\lambda}$ stand for the transmittance of bleached and colored samples, respectively. Coloration efficiency (CE, η) is defined as the ratio of change of optical density (ΔOD_λ) at corresponding injected/ejected charge density (Q_{in}) per unit area (S), which is described as follows:

$$\eta = \Delta OD_\lambda / Q_{in} \quad (2)$$

$$Q_{in} = \int i dt / S \quad (3)$$

Obviously, both OD and CE present the ability of optical modulation during the coloration-bleaching process but the latter one is under the considering of energy consumption. In principle, both OD and CE result from the variation of films' absorption. Fig. 5 shows the precise comparison of OD and CE between dense and macroporous WO_3 films. Just as previously reported [3,21–23], dense WO_3 films show high OD or CE in the visible band but relatively low in the near IR. Surprisingly, it is found that orthogonal characteristic of EC performance could be achieved for the ordered macroporous films. This reasoning behind it includes two parts: an enhancement in the long wave band and suppression in short wave region of modulation of lights, which seems to originate from the ordered macroporous structures.

In the short wave region, the wavelength of incident lights is close to the characteristic size of cavities on the surface of macroporous films. The surface of films can be considered as a rough surface, which greatly enhances the Mie scattering. The photonic bandgap effect is also present due to the ordered structure, which enhances the Bragg scattering. As a result, light which gets access to the inside macroporous films at colored or bleached state is significantly reduced, i.e. the absorption of films is greatly decreased. OD or CE is consequently depressed due to the macroporous structure. With the increasing of incident wavelength, Mie or Bragg scattering would decrease. Fig. 6 shows the schematic illustration of conduction of ions/electrons and transmission of lights in ordered macroporous films. The interconnected porous structure provides the great area between electrolyte and tungsten oxide. The continuous wall structure provides the pathway for electron conduction and shortens the length of diffusion path. Moreover, lights would have multiple refractions inside of ordered macroporous WO_3 films due to the multi-layers of connected macropores. The propagation path of light is thereby extended, which leads to great increase of the absorption and eventually the ability of light modulation. These two sides cause the enhancement of electrochromic performance in the near IR bands.

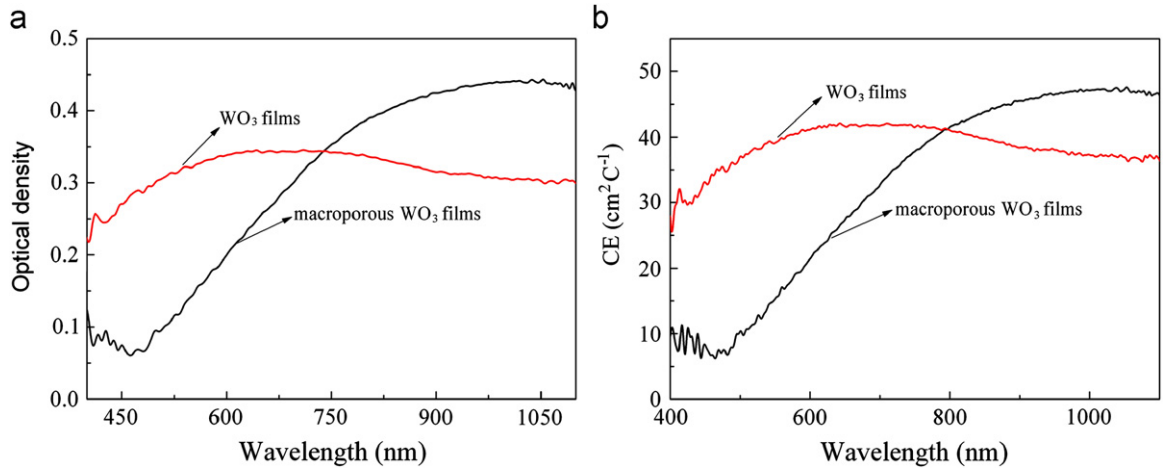

Fig. 5. Optical density and coloration efficiency of WO_3 films (*a*) and ordered macroporous films (*b*).

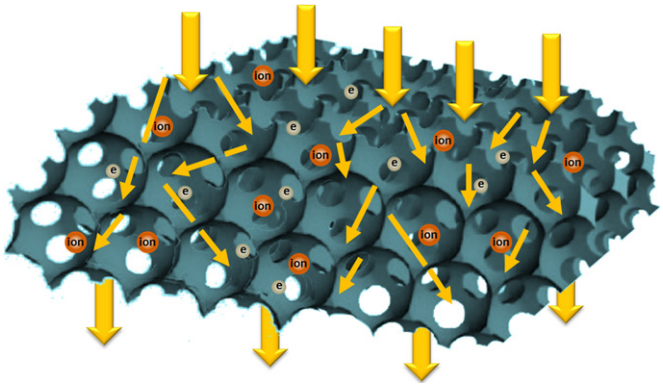

Fig. 6. Schematic bicontinuous electron/ion conducting and lights transmission structure of 3DOM WO_3 films.

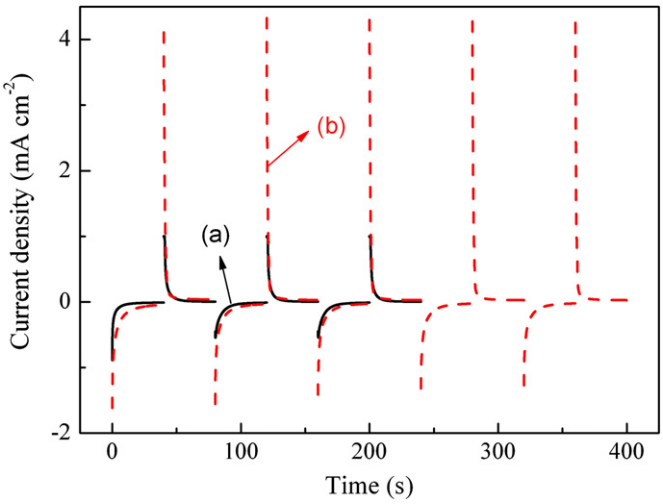

Fig. 7. Coloration-bleaching characteristics in WO_3 films (*a*) and ordered macroporous films (*b*).

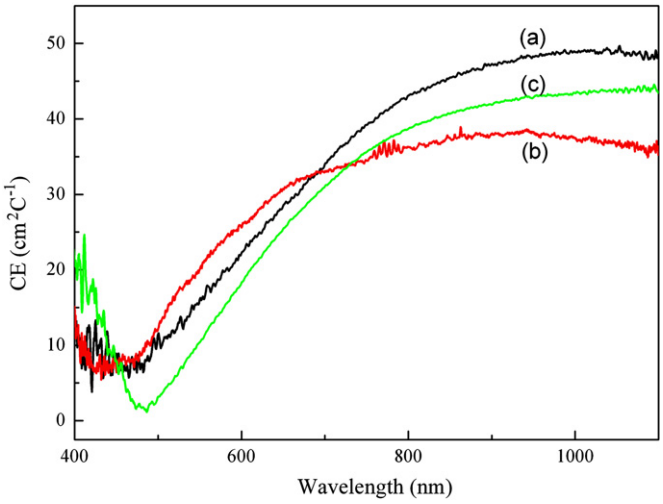

Fig. 8. CE curve of ordered macroporous WO_3 films with different pore sizes of 325 nm (*a*), 410 nm (*b*) and 620 nm (*c*).

The EC response time is another important parameter. Fig. 7 shows the current versus. time during the coloration-bleaching process through the step method. Combining with the change of transmittance, the response times for coloration and bleaching are obtained to be 5.19 s and 8.76 s, respectively. It is noticeably shorter than those of dense films, namely 6.9 s and 11.8 s. It is widely accepted that the electrochromic response time is actually limited by two factors: the ion diffusion coefficient and the length of diffusion path [24]. The former one depends on the chemical structure while the latter depends on the microstructure.

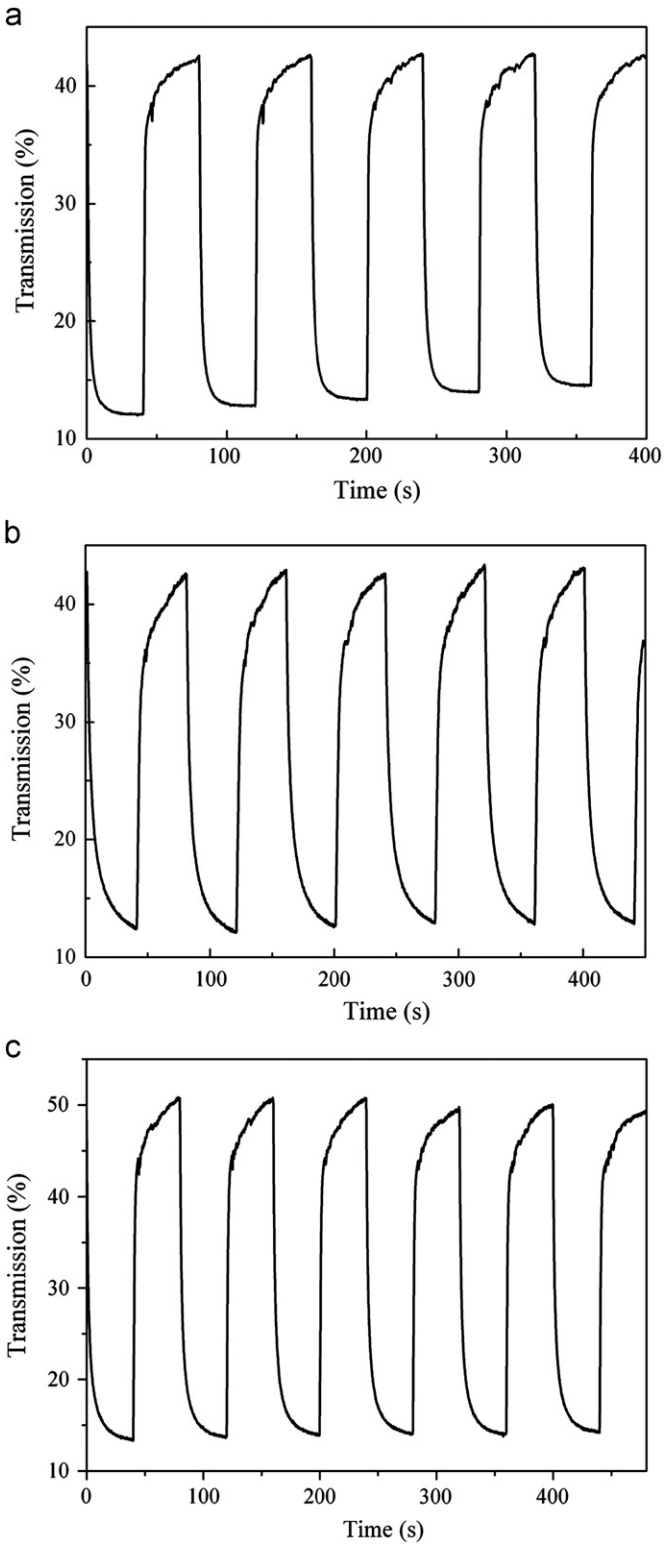

Fig. 9. Coloration-bleaching characteristics in 3DOM WO_3 films at 800 nm with different pore sizes of 325 nm (*a*), 410 nm (*b*) and 620 nm (*c*).

Table 1
Electrochromic characteristics of ordered macroporous WO_3 thin films.

Pore size (nm)	Maximum CE ($cm^2\ C^{-1}$)	Coloration time (s)	Bleaching time (s)
325	50.18	5.19	8.76
410	38.94	8.34	13.14
620	44.97	8.14	12.90

Under the same preparation conditions, the chemical structures of macroporous WO_3 films could be considered to be similar to the dense films. Therefore, the effect of macroporous structure on the EC performance is governed by the change of diffusion path due to the macroporous structure. It has been well proved that porous materials have fast response time due to the greater surface area [10,11,14,22]. Different from general porous materials, here 3DOM structure has the uniformly distributed, open and connected channels. This structure is much good for the diffusion of ions into the materials, which decreases the response time.

3.3. Influence of pore size on the electrochromic performance

Three macroporous films with different pore sizes are chosen to further investigate the effect on their electrochromic performance. Their CE and coloration-bleaching curves are shown in Figs. 8 and 9, respectively. Table 1 summarizes the maximum CE and corresponding response time. The ordered macroporous films with three different pore sizes exhibit very different EC performance. The macroporous film with the smallest size of pores has the best EC properties, followed by the sample with the biggest size of pores.

The nonlinear relationship between the pore size and the EC performance manifests in at least two aspects. On one hand, it is obvious that there are more layers of connected macroporous structures for 3DOM materials with smaller pores. The above analysis demonstrates stronger refraction and longer propagation paths for the light beam within the 3DOM materials. Thus, the absorption in either coloration or bleaching state is enhanced, and both OD and CE are improved. On another side, the infiltration of WO_3 into the void spaces is much more favorable during the sol–gel process with the increase of sphere size, resulting in better integrity of macroporous structures. Thus both the layer number and the perfection of macroporous structure benefit for the optical modulation for 3DOM electrochromic materials. It is also found that the response time has the same trend as the CE. For 3DOM WO_3 films with the smallest pore size, largest surface area and thinnest walls are derived to improve the ion/electron diffusion. For the sample with the pore size of 620 nm, the structural integrity should play an important role leading to better penetration of ions into the 3DOM WO_3 framework.

4. Conclusions

Ordered macroporous tungsten oxide films are fabricated through the template-assisted sol–gel method and their EC performance were investigated in comparison with nonporous films or those with different pore sizes. The improved EC performance of ordered macroporous WO_3 films results from three structural features: ordered structure, multi-layer interconnected pores and surface geometric morphologies. The ordered structure gives the photonic bandgap performance, and interconnected pores not only provide a continuous pathway for electron/ion conduction but also increase the opportunities for lights′ multiple refraction of interior layer. While the surface geometric morphologies enable Mie plasmon interaction in the top layer of the structure. This originates from the interaction between ordered macroporous materials and light under the condition of insertion/extraction of ions/electrons, which also provides the special electrochromic performance for ordered macroporous WO_3 films. Small pore size and perfection of macroporous structures are much favorable in the conduction of ions/electrons but also to the transmission of light. The electrochromic performance is also related with the film thickness which is to be further studied.

Acknowledgments

This work is supported by the Program National Natural Science Foundation (nos. 51010005, 90916020, 51174063 and 51102068), the Program for New Century Excellent Talents in University (NCET-08-0168), the National Postdoctoral Foundation (20100471033) and the Fundamental Research Funds for the Central Universities (Grant no. HIT.ICRST.2010001 & HIT.NSRIF.2010034) and Sino-German joint project (GZ550).

References

[1] C.M. Lampert, Electrochromic materials and devices for energy efficient windows, Solar Energy Materials 11 (1984) 1–27.
[2] J. Livage, D. Ganguli, Sol–gel electrochromic coatings and devices: a review, Solar Energy Materials 68 (2001) 365–381.
[3] S.K. Deb, Opportunities and challenges in science and technology of WO_3 for electrochromic and related applications, Solar Energy Materials Solar Cells 92 (2008) 245–258.
[4] C.M. Lampert, C.G. Granqvist, Large area chromogenics: materials and device for transmittance control, SPIE Institutes for Advanced Optical Technologies (1998). IS4.
[5] C.G. Granqvist, Handbook of Inorganic Electrochromic Materials, Elsevier, Amsterdam, 1995.
[6] J.S. Hale, J.A. Woollam, Prospects for infrared emissivity control using electrochromic structures, Thin Solid Films 339 (1999) 174–180.
[7] K. Sauvet, A. Rougier, L. Sauques, Electrochromic WO_3 thin films active in the IR region, Solar Energy Materials Solar Cells 92 (2008) 209–215.
[8] A. Rougier, K. Sauvet, L. Sauques, Towards electrochromic devices active in the IR region, Smart Materials Energy Communications Security (2008) 41–51.
[9] K. Sauvet, L. Sauques, A. Rougier, IR electrochromic WO_3 thin films: from optimization to devices, Solar Energy Materials Solar Cells 93 (2009) 2045–2049.
[10] H.S. Shim, J.W. Kim, Y.E. Sung, Electrochromic properties of tungsten oxide nanowries fabricated by electrospinning method, Solar Energy Materials Solar Cells 93 (2009) 2062–2068.
[11] P.M. Kadam, N.L. Tarwal, P.S. Shinde, R.S. Patil, H.P. Deshumkh, P.S. Patil, From beads-to-wires-to-fibers of tungsten oxide: electrochromic response, Applied Physics A 97 (2009) 323–330.
[12] E. Yablonovitch, Inhibited spontaneous emission in solid-state physics and electronics, Physical Review Letters 58 (1987) 2059–2062.
[13] S. John, Strong localization of photons in certain disordered dielectric superlattices, Physical Review Letters 58 (1987) 2486–2489.
[14] T. Sumida, Y. Wada, T. Kitamura, S. Yanagida, Electrochemical change of the photonic stop band of the ordered macroporous WO_3 films, Chemistry Letters (2002) 180–181.
[15] S.L. Kuai, G. Bader, P.V. Ashrit, Tunable electrochromic photonic crystals, Applied Physics Letters 86 (2005). 221110-221110-3.
[16] M. Sadakane, K. Sasaki, H. Kunioku, B. Ohtani, R. Abe, W. Ueda, Preparation of 3D ordered macroporous tungsten oxide and nano-crystalline particulate tungsten oxides using a colloidal crystal template method, and their structural characterization and application as photocatalysts under visible light irradiation, Journal of Materials Chemistry 20 (2010) 1811–1818.
[17] U.O. Krasovec, B. Orel, A. Georg, V. Wittwer, The gasochromic properties of sol–gel WO_3 films with sputtered Pt catalyst, Solar Energy 68 (2000) 541–551.
[18] M.A. Mclachlan, N.P. Johnson, R.M. Rue, La De, D.W. McComb, Thin film photonic crystals: synthesis and characterisation, Journal of Materials Chemistry 14 (2004) 144–150.
[19] A. Temmink, O. Anderson, K. Bange, H. Hantsche, X. Yu, Optical absorption of amorphous WO_3 and binding state of tungsten, Thin Solid Films 192 (1990) 211–218.

[20] E. Ozkan, S.H. Lee, C.E. Tracy, F.Z. Tepchan, J.R. Pitts, S.K. Deb, Comparison of electrochromic amorphous and crystalline tungsten oxide films, Solar Energy Materials Solar Cells 79 (2003) 439–448.
[21] T. Brezesinski, D.F. Rohlfing, S. Sallard, M. Antonietti, B.M. Smarsly, Highly crystalline WO_3 thin films with ordered 3D mesoporosity and improved electrochromic performance, Small 2 (2006) 1203–1211.
[22] Y.F. Yuan, X.H. Xia, J.B. Wu, et al., Enhanced electrochromic properties of ordered porous nickel oxide thin film prepared by self-assembled colloidal crystal template-assisted electrodeposition, Electrochimica Acta 56 (2011) 1208–1212.
[23] M. Deepa, P. Singh, S.N. Sharma, S.A. Agnihotry, Effect of humidity on structure and electrochromic properties of sol–gel-derived tungsten oxide films, Solar Energy Materials Solar Cells 90 (2006) 2665–2682.
[24] S.H. Lee, R. Deshpande, P.A. Parilla, K.M. Jones, B. To, A.H. Mahan, A.C. Dillon, Crystalline WO_3 nanoporous for highly improved electrochromic applications, Advanced Materials 18 (2006) 763–766.